An analytical approach to 3D orthodontic load systems

Thomas R. Katona[a], **Serkis C. Isikbay**[b], and **Jie Chen**[c]

[a]Associate Professor, Department of Orthodontics and Oral Facial Genetics, Indiana University School of Dentistry, and Department of Mechanical Engineering, Purdue University School of Engineering and Technology, Indianapolis, Ind

[b]Private practice, Speedway, Ind

[c]Professor, Department of Mechanical Engineering, Purdue University School of Engineering and Technology, and Department of Orthodontics and Oral Facial Genetics, Indiana University School of Dentistry, Indianapolis, Ind

Abstract

Objective—To present and demonstrate a pseudo three-dimensional (3D) analytical approach for the characterization of orthodontic load (force and moment) systems.

Materials and Methods—Previously measured 3D load systems were evaluated and compared using the traditional two-dimensional (2D) plane approach and the newly proposed vector method.

Results—Although both methods demonstrated that the loop designs were not ideal for translatory space closure, they did so for entirely different and conflicting reasons.

Conclusions—The traditional 2D approach to the analysis of 3D load systems is flawed, but the established 2D orthodontic concepts can be substantially preserved and adapted to 3D with the use of a modified coordinate system that is aligned with the desired tooth translation.

Keywords

Three-dimensional; Orthodontic force systems; Biomechanics; T-loop archwire; Moment-to-force ratio

INTRODUCTION

Orthodontic load (force and moment) systems are traditionally quantified as plane two-dimensional (2D) arrangements.[1–7] Three-dimensional (3D) systems have typically been viewed as combinations of three such 2D planes oriented in each tooth's facial/buccal, incisal/occlusal and mesiodistal directions. But 3D engenders more complex interactions.[7–9] Therefore, a purpose of this paper is to show that the loads in the 2D planes are not independent, and therefore, their actions should not be uncoupled and treated separately because that leads to errors in the prediction of orthodontic displacements. The second

Corresponding author: Dr Thomas R. Katona, Indiana University School of Dentistry, IUPUI, 1121 W Michigan St, Indianapolis, IN 46202 (tkatona@iu.edu).

purpose is to present a pseudo-3D analytical approach that substantially preserves the concepts and nomenclature of the accepted 2D methods. Finally, the third purpose is to show experimental results used to demonstrate and contrast the analyses.

Consider, as viewed in the traditional 2D analytical approach, the translations of a maxillary left lateral incisor and canine into an extraction space. As observed in the occlusal plane (Figure 1), there are three pertinent coordinate systems. X-Y is the global system and there are two *x-y* systems associated with the respective buccal and distal sides of each tooth. Z and *z* are in the superior/apical direction. Thus, X-Y and the two *x-y* define the occlusal plane. (X-Z defines the midsagittal plane and Y-Z defines a frontal plane.)

The most general 3D load system that a loop can apply to a bracket consists of three force and three moment components (Figure 2a). In the typical traditional 2D approach, this 3D load system is independently analyzed in tooth-relative orthogonal planes formed by the *x-y*, *y-z,* and *x-z* axes of each tooth (Figure 1). In the *y-z* plane (Figures 1b and 2a), the force components are F_y and F_z, and the moment component, $\pm M_x$, acts in the buccal/palatal direction (according to the right-hand-rule [RHR] convention) to compensate for second order rotation. Third order tipping takes place in the *x-z* plane with F_x, F_z, and M_y. And, in the *x-y* (occlusal) plane, the forces are F_x and F_y, and M_z is associated with mesial-in/distal-out rotation. Thus, the most general 2D model contains only two of the three force components, and only one of the three moment components.

To associate a load system on the bracket with the resulting tooth displacement, the tooth's center of resistance (CRes) is taken into account. CRes is an imaginary point fixed relative to the tooth, that, if a force were applied to it, the tooth would undergo pure translation in the direction of that force. (An alternative definition is that the tooth undergoes pure rotation about CRes if only the moment of a couple is applied to the tooth.) The location of CRes is determined by the shapes and the mechanical properties of the root, socket, and periodontal ligament matrix and fibers.[10–12] In a single rooted tooth, it is somewhere within the middle third of the root.

Thus, viewed in 2D, for the space-closing translation of the lateral incisor, a force in its distal direction (F_y) would have to be applied to its CRes (Figure 3a). At the bracket, the equivalent load system consists of the same F_y plus a moment, $-M_x$ (Figure 3b,c). The magnitude of M_x should be (F_y) (d_z) where d_z, the moment arm, is the distance between CRes and the line-of-action (LOA) of F_y (Figure 3a). Thus, for distal translation of the tooth, the moment-to-force ratio (M/F) that has to be applied to the bracket by the appliance is M_x/F_y (= d_z). In effect, $-M_x$ serves to eliminate the second order rotation caused by moving F_y from CRes to the bracket. Second order gable bends are often used to augment insufficient loop-generated M_x/F_y values.

In total, there are nine M/F ratio permutations, but because forces cannot generate moments in their own directions (as defined by the RHR), the crossed-out quantities have no meaning. In the customary 2D segmental view of space closure (Figures 1 through 6), the emphasis is on F_y because it is the force component in the desired tooth movement direction and because it has the longest (8–10 mm) moment arm (d_z) relative to CRes. That combination produces

a substantial second order tipping moment about CRes so its counteraction (with M_x) has been the traditional focus of loop design and gable bend studies aimed at increasing M_x/F_y to the necessary 8–10 mm magnitude.[13] (The generic "moment-to-force ratio" in the literature usually refers implicitly to M_x/F_y.)

An analytical method should be applicable to the most general loading (Figure 2a). Therefore, the effects of all forces, moments, and M/F ratios must be taken into account. In the plane discussed above (Figure 3), another $\pm M_x$ component can be produced by the intrusive/extrusive force component ($\pm F_z$) on the bracket (Figure 4), which must be opposed by an applied M_x/F_z that is equal to d_y, the distance (ie, the moment arm) between CRes and the LOA of F_z. However, in actuality, in this plane, the M_x that is applied to the tooth by the appliance must negate the net M_x on the tooth that is produced by the combined actions of F_y and F_z (Figures 3 and 4). Perhaps because d_y is relatively small when an upright tooth is translated, and because F_z is also relatively small, the contribution of F_z is usually ignored.

In the occlusal plane, the same F_y that produces an M_x (Figure 3) also produces an M_z (mesial-out, distal-in rotation) (Figure 5a). That moment must be counteracted by a $-M_z$ (= $F_y d_x$) that is generated by the loop. Another M_z is produced by F_x, and it must be negated by an M_z/F_x that is equal to d_y (Figure 5b). But, analogous to the y-z plane (Figures 3 and 4), the appliance-applied M/F in this plane must counteract the net M_z produced by F_y (Figure 5a) and F_x (Figure 5b). And finally, M_y moment ("torque") in the x-z plane is produced by F_x and F_z due to their respective moment arms, d_z and d_x (Figure 6).

Thus, a force component can produce moments in the two directions that are perpendicular to it, or a moment component can be created by force components in the other two directions (Figure 7). Therefore, the separation of the complex 3D phenomena into three simpler 2D models can create problems because, in reality, those 2D models are not independent of each other. Change in one plane, a gable bend for example, has the potential to impart changes in the other two planes.

The above discussions have been limited to the traditional 2D analysis, and therefore, to tooth translations and rotations relative to their individual x-y-z (buccal-distal-apical) coordinate systems. In 3D scenarios involving the arch, this can present severe shortcomings because the orientation of x-y-z for each tooth is different relative to each other and relative to the global system (Figure 1a). Therefore, unlike the components shown in Figure 2a, a distal force component on the lateral incisor, $+F_y$, is not in the opposite direction to a mesial force component on the canine, $-F_y$. Thus, concepts based on Figure 2a are applicable to the unrealistically distorted arches in Figure 2b or c.

MATERIALS AND METHODS

It is proposed that for the purposes of analyzing and characterizing 3D orthodontic load systems, the analysis be conducted in coordinate systems that are more closely aligned with the approximated directions of desired translations, the y' in Figure 8. By so doing and slightly modifying the nomenclature of the above described conventional x-y-z based 2D

systems, mainstream orthodontic concepts and approaches can be salvaged and adapted to 3D.

Using the analyses of load systems in a simulated translatory space closure, the proposed and traditional methods are compared. Zero-, 1-, and 2-mm activation results from 2 of the 16 loop designs, configurations no. 13 and no. 8 in the previous publication,[7] are used as exemplars.

First, it is estimated that the incisor and canine x-y axes are rotated 30° and 65°, respectively, relative to X-Y (Figure 1a). Then, with transformation equations,[14] the x-y system load components are projected onto the X-Y global system and defined on each tooth as $\mathbf{F}_G$ and $\mathbf{M}_G$ (Figure 9). Then, it can be ascertained if the $\mathbf{F}_G$ forces act along their respective desired (y') directions, estimated as approximately 50° and 35°. If deemed acceptable, the $\mathbf{M}_G$ must have components, $M_\perp$, that are perpendicular to $\mathbf{F}_G$, with the appropriate senses and $M_\perp/F_G$ ratios to prevent unwanted tipping (Figure 9b).

RESULTS

For the first loop design, the load systems on the brackets are presented traditionally in each tooth's respective x-y-z system (Figure 10). The same data are shown according to the proposed method in Figure 11. The other loop design results are depicted in Figure 12.

DISCUSSION

A purpose of this project is to illustrate the differences, advantages, and deficiencies of the two approaches when applied to the identical experimental measurements. The traditional presentation of data (Figure 10) presents critical pitfalls when extrapolated to 3D mainly because the desired tooth displacements rarely coincide with the x-y-z coordinate system of a tooth and because the two x-y-z systems are not aligned. Thus, 3D interactions are better handled vectorially, as proposed.

An acceptable load system should produce the intended tooth displacements (in this case, translation into the extraction space) with minimal side effects. According to the conventional 2D approach, for space closing translation of the incisor, the following conditions are required: the force should be distally directed ($F_y > 0$) and the moment should be in the palatal direction ($M_x < 0$) (Figure 2), with M_x/F_y between −8 and −10 mm. Concomitantly, on the canine, the force should be mesial ($F_y < 0$), and the moment should be buccally directed ($M_x > 0$), and M_x/F_y should be between −8 and −10 mm. With the first loop configuration, at 1- and 2-mm activation, $-10 < M_x/F_y < -8$ is produced on the canine (Figure 10d). The $F_y < 0$ and $M_x > 0$ requirements are also met (Figure 10c,d). However, this loop wreaks havoc on the incisor, with M_x/F_y equal to −62.0 and −109.0 mm, respectively, at the 1- and 2-mm activations. When viewed in the occlusal plane (Figure 11), the inappropriate force directions are immediately obvious.

Thus, 3D analysis can be manageably performed for each tooth by vectorially adding its F_x and F_y, and its M_x and M_y, and expressing the sums in the global X-Y system as $\mathbf{F}_G$ and $\mathbf{M}_G$ for each tooth (Figures 9, 11, and 12). Then it becomes possible to apply the following

requirements, in any sequence, for a suitable translatory space closing load system (Figure 9):

- R1: The force vector, $\mathbf{F}_G$, must be in the required translatory direction;

- R2: The associated moment vector ($\mathbf{M}_G$) must have a component ($M_\perp$) in the appropriate direction, ie, perpendicular to $\mathbf{F}_G$ and with the correct sense as defined by the RHR;

- R3: The required $M_\perp/F_G$ ratio must be met;

- R4: The magnitude of $\mathbf{F}_G$ must be within some suitably defined range;

- R5: Load components F_z and M_z must be within defined acceptable ranges; and

- R6: $M_\parallel$, the component of $\mathbf{M}_G$ that is parallel to $\mathbf{F}_G$ (Figure 9b), hence perpendicular to $M_\perp$, must be sufficiently small.

If any requirement is violated on either tooth, then all other conditions are beside the point. (These requirements are entirely independent of the orthodontic appliance.) The evaluation process is illustrated as follows:

On the canine, the second spring configuration produces acceptable force directions at 1 and 2 mm of activation (Figure 12b), thus meeting condition R1. Their respective $M_\perp/F_G$ are −11.1 and −9.6 mm. (The traditional M_x/F_y are −12.1 and −19.1 mm, respectively.) Thus, at 1-mm activation, the force direction is optimal, but the $M_\perp/F_G$ ratio is out of range, thereby violating condition R3. Although the 2-mm activation satisfies requirements R1, R2, and R3, R6 is questionable because $\mathbf{M}_G$ has a relatively large $M_\parallel$ component that would cause a substantial *modified* third order rotation. ("Modified" because the crown tips not only in the traditional palatal direction, but also toward the distal.) But, assuming for the sake of argument that R6 is acceptable, condition R5 must be examined. The roles of F_z (intrusion/extrusion) and M_z (mesial-in/distal-out rotation) in this analysis are exactly as they are in the traditional approach. Note the concomitant gross violations of R1 on the incisor in Figure 12a.

The proposed approach eliminates the use of $\mathbf{F}_G$ whose directions are deemed unacceptable. This simplifies the analysis because there is no analogous $\pm F_{x'}$ force component. Further simplification of the 3D analysis is possible. Figure 8b shows the assumption of collinear paths of the two teeth along the y″-axis. So, instead of performing the traditional individual analyses in the *x-y-z* coordinate systems of each tooth (Figure 1a), analyses can be done in their *x′-y′-z* systems. This replicates the traditional approach depicted in Figures 2 through 6. Thus, in effect, an appropriate $\mathbf{F}_G$ is analogous to F_y in the traditional approach and $M_\perp$ is analogous to M_x. The magnitudes and directions of $F_{x''}$ and $M_\parallel$ (which is analogous to M_y) indicate the level of potential unwanted side effects, another advantage of this approach.

The requirements for translation, the illustrative example, are listed above as R1 to R6. But the proposed approach is adaptable to any tooth displacement if the requirements are appropriately modified. In all cases, the $\mathbf{F}_G$ must be in the direction of desired translation and the M/F ratios must be specified for the desired rotations and tipping, just as with the

conventional approach. The essential difference is that the analyses are performed relative to the y', not y.

The analyses illustrate the intricate nonintuitive confounding effects of 3D. The well-defined concepts and principles of 2D mechanics (Figures 2 through 6) cannot be directly extrapolated to curved-arch 3D, and the two analytical methods attribute loop failure to different reasons. (For the purposes of comparing the analytical approaches, loop design is irrelevant.) Although far from a panacea, the proposed displacement- relative analysis allows for established 2D concepts to be applied in 3D.

CONCLUSIONS

- The traditional 2D approach to the analysis of 3D load systems is flawed.

- Traditional 2D orthodontic concepts can be adapted to a pseudo-3D analysis with the use of a modified coordinate system that is aligned with the desired tooth translation direction.

Acknowledgments

References

1. Chen J, Bulucea I, Katona TR, Ofner S. Complete orthodontic load systems on teeth in a continuous full archwire: the role of triangular loop position. Am J Orthod Dentofacial Orthop. 2007; 132:143, e141–148. [PubMed: 17693357]

2. Chen J, Markham DL, Katona TR. Effects of T-loop geometry on its forces and moments. Angle Orthod. 2000; 70:48–51. [PubMed: 10730675]

3. Gregg, J.; Chen, J. The effect of wire fixation methods on the measured loading systems of a T-loop orthodontics spring. Paper presented at: AAO Annual Meeting; Month DD, 1997; Philadelphia, Pa.

4. Katona TR, Le YP, Chen J. The effects of first- and second-order gable bends on forces and moments generated by triangular loops. Am J Orthod Dentofacial Orthop. 2006; 129:54–59. [PubMed: 16443479]

5. Lisniewska-Machorowska B, Cannon J, Williams S, Bantleon HP. Evaluation of force systems from a "free-end" force system. Am J Orthod Dentofacial Orthop. 2008; 133:791, e1–10. [PubMed: 18538238]

6. Raboud D, Faulkner G, Lipsett B, Haberstock D. Three-dimensional force systems from vertically activated orthodontic loops. Am J Orthod Dentofacial Orthop. 2001; 119:21–29. [PubMed: 11174536]

7. Katona TR, Isikbay SC, Chen J. Effects of first- and second-order gable bends on the orthodontic load systems produced by T-loop archwires. Angle Orthod. 2013 Aug 29. Epub ahead of print.

8. Badawi HM, Toogood RW, Carey JP, Heo G, Major PW. Three-dimensional orthodontic force measurements. Am J Orthod Dentofacial Orthop. 2009; 136:518–528. [PubMed: 19815153]

9. Chen J, Isikbay SC, Brizendine EJ. Quantification of three-dimensional orthodontic force systems of T-loop archwires. Angle Orthod. 2010; 80:754–758.

10. Qian H, Chen J, Katona TR. The influence of PDL principal fibers in a 3-dimensional analysis of orthodontic tooth movement. Am J Orthod Dentofacial Orthop. 2001; 120:272–279. [PubMed: 11552126]

11. Meyer BN, Chen J, Katona TR. Does the center of resistance depend on the direction of tooth movement? Am J Orthod Dentofacial Orthop. 2010; 137:354–361. [PubMed: 20197172]

12. Viecilli RF, Budiman A, Burstone CJ. Axes of resistance for tooth movement: does the center of resistance exist in 3-dimensional space? Am J Orthod Dentofacial Orthop. 2013; 143:163–172. [PubMed: 23374922]

13. Proffit, WR.; Fields, HW.; Sarver, DM. Contemporary Orthodontics. 4. Chicago, Ill: CV Mosby; 2007.

14. Beer, FP.; Johnston, ER.; Eisenberg, ER. Vector Mechanics for Engineers - Statics. 8. Boston, Mass: McGraw-Hill; 2007.
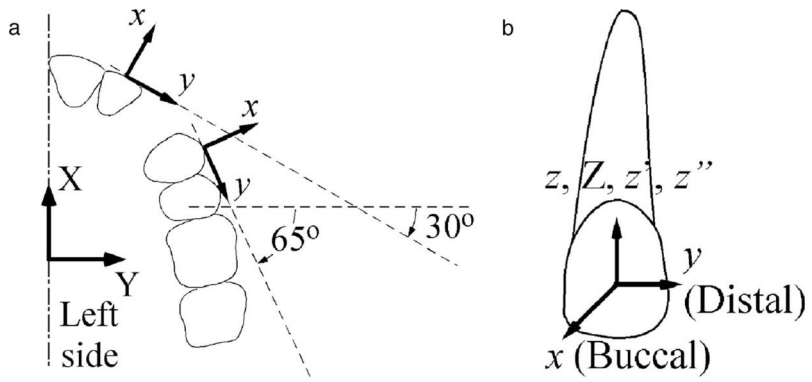
Figure 1.
(a) Occlusal view of the simulated clinical case showing the global (X-Y) and the estimated local (*x-y*) coordinate systems on the maxillary lateral incisor (approximately 30°) and the canine (approximately 65°) brackets. (b) The *x-y-z* axes of the lateral incisor bracket.
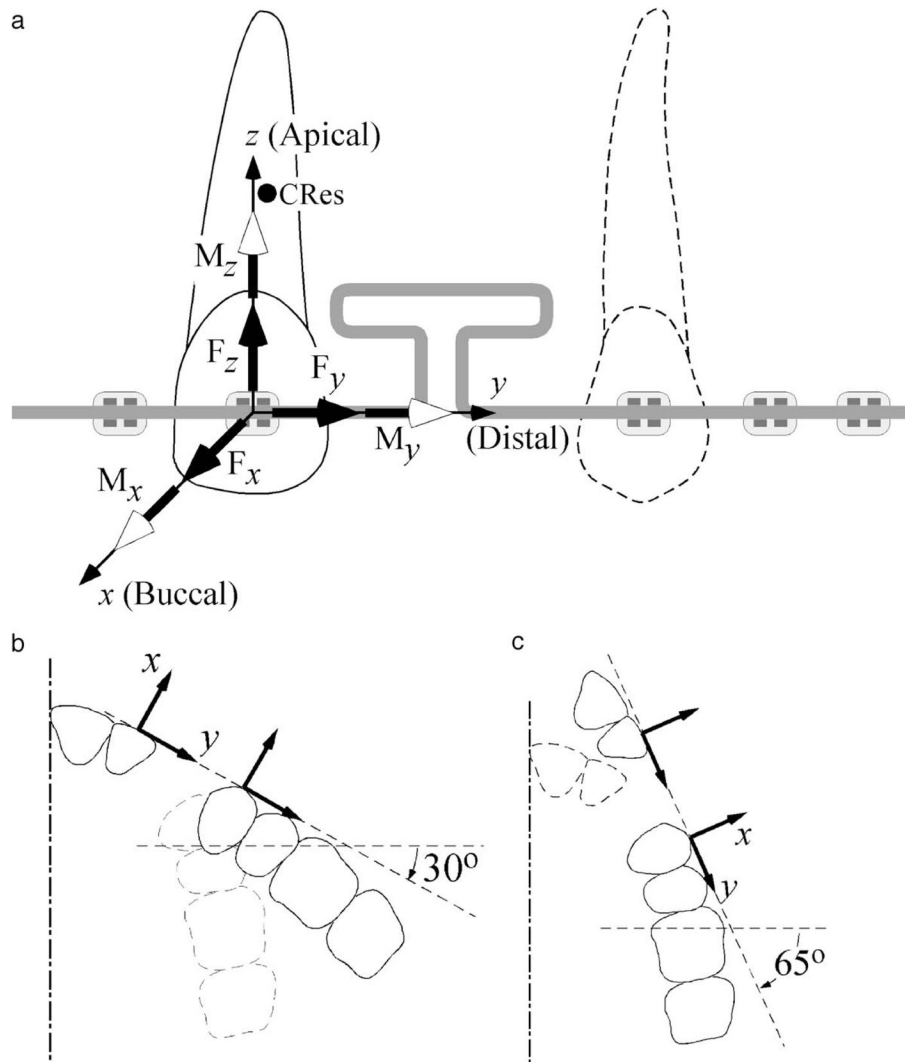
Figure 2.
(a) Schematic of complete generic load system acting on a maxillary left lateral incisor bracket. $\pm Fx$, $\pm Fy$, and $\pm Fz$ force components act in the buccal/palatal, distal/mesial, and apical/incisal directions, respectively. The directions of the moment vector components ($\pm Mx$, $\pm My$, and $\pm Mz$) are defined by the RHR convention—the thumb of the right hand points in the direction of the moment (open) vector arrow, and the fingers indicate the direction of rotation. As an example, $-Mz$ would produce a mesial-in distal-out rotation. (b) The distorted arch corresponds to the depictions in Figure 2a and in Figure 1a. (c) Distorted arch based on canine x-y data.
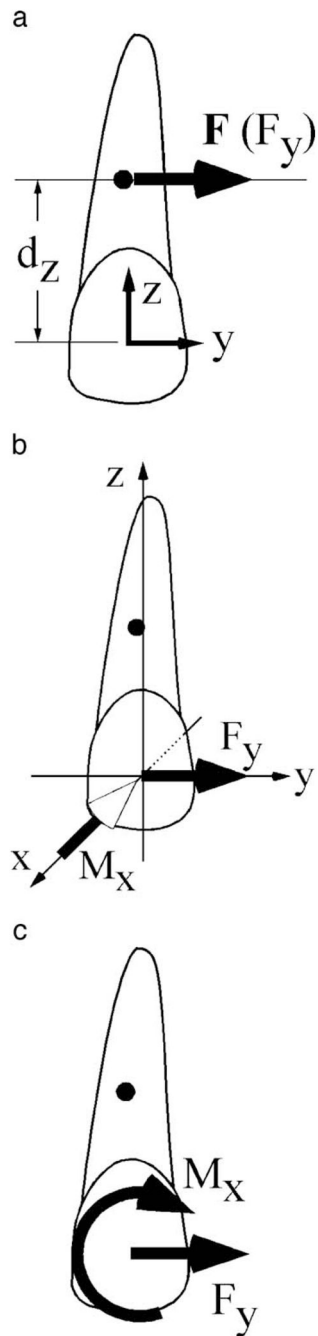
Figure 3.
Load systems required for distal translation applied at (a) CRes or at (b and c) the bracket. b and c use, respectively, the RHR and the more (dentally) conventional depictions.
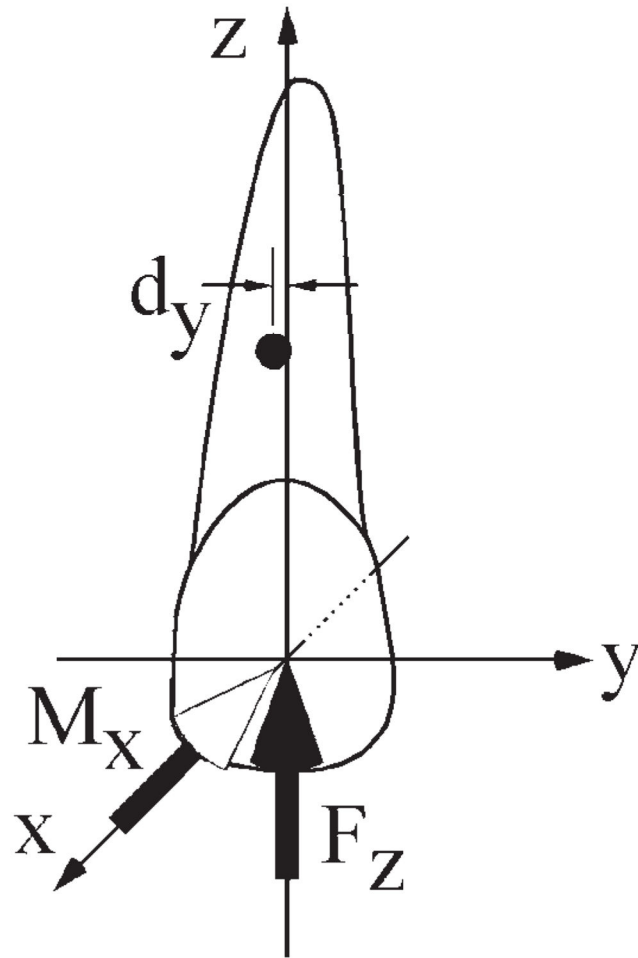
Figure 4.
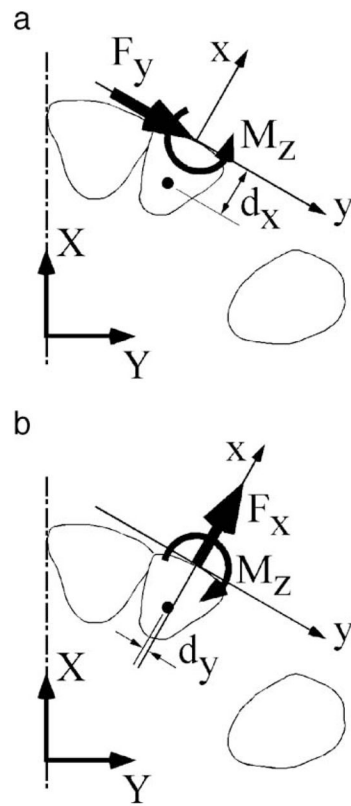For translation, M*x* also counters the second order rotation produced by F*z*.

Figure 5.
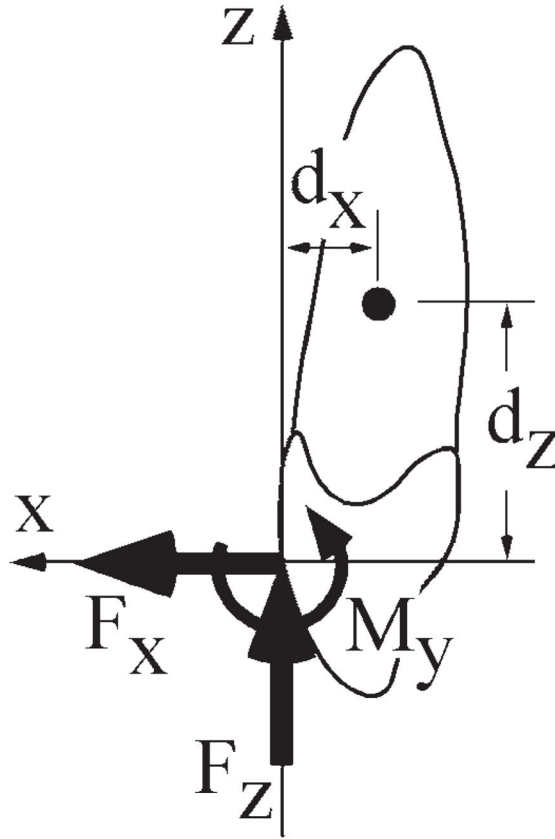$Mz = -Fydx + Fxdy$ to prevent rotations produced by (a) Fy and (b) Fx.

Figure 6.
M*y* is applied to prevent third order rotation produced by F*x* and F*z* in the *x-z* plane. M*y* = F*x*d*z* + F*z*d*x*.

$$F_x \qquad M_x$$
$$F_y \qquad M_y$$
$$F_z \qquad M_z$$
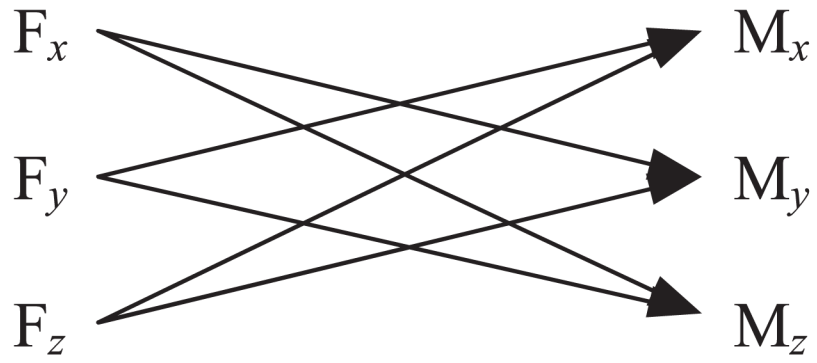
Figure 7.
Each force component can generate two moment components. Each moment component can be generated by two force components.
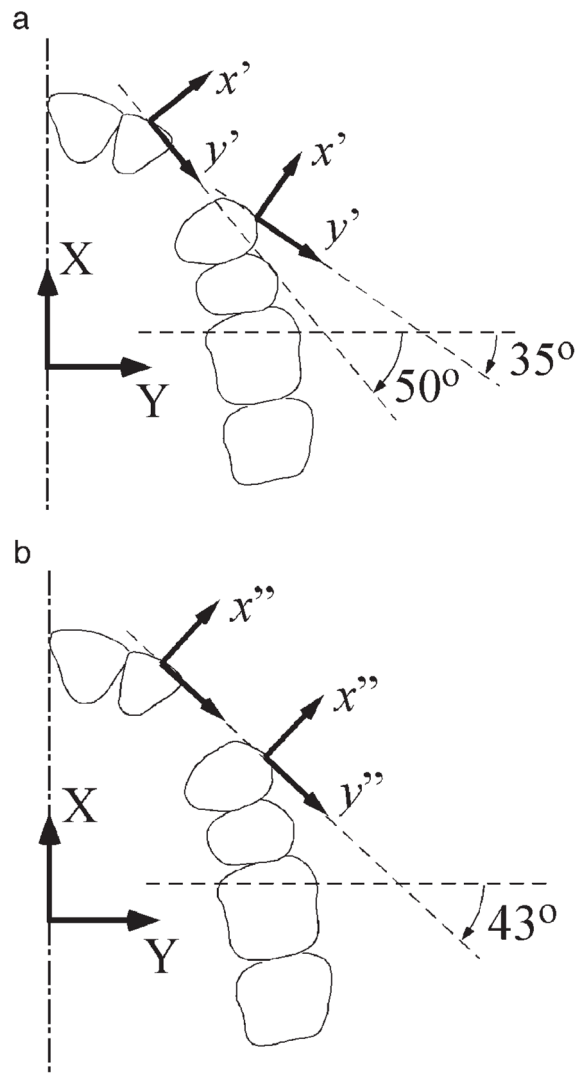
Figure 8.
(a) Instead of traditional analyses in the two *x-y* coordinate systems (Figures 1 through 6), it is proposed that analyses be performed in the two *x′-y′* systems in which the *y′*-axes are more closely aligned (approximately 50° instead of approximately 30° for the incisor and approximately 35° instead of approximately 65° for the premolar) with the direction of desired tooth translations. (b) Analogous to Figure 2a, the assumption that the two y′-axes are collinear yields the y″-axis. Its angulation, 43°, is the average of the 35° and the 50°. (Alternatively, the 43° approximates the line joining the two brackets.) With this approximation, the gross arch distortion (Figure 2b) is avoided, and the traditional widely accepted concepts associated with Figure 2a are more acceptable.
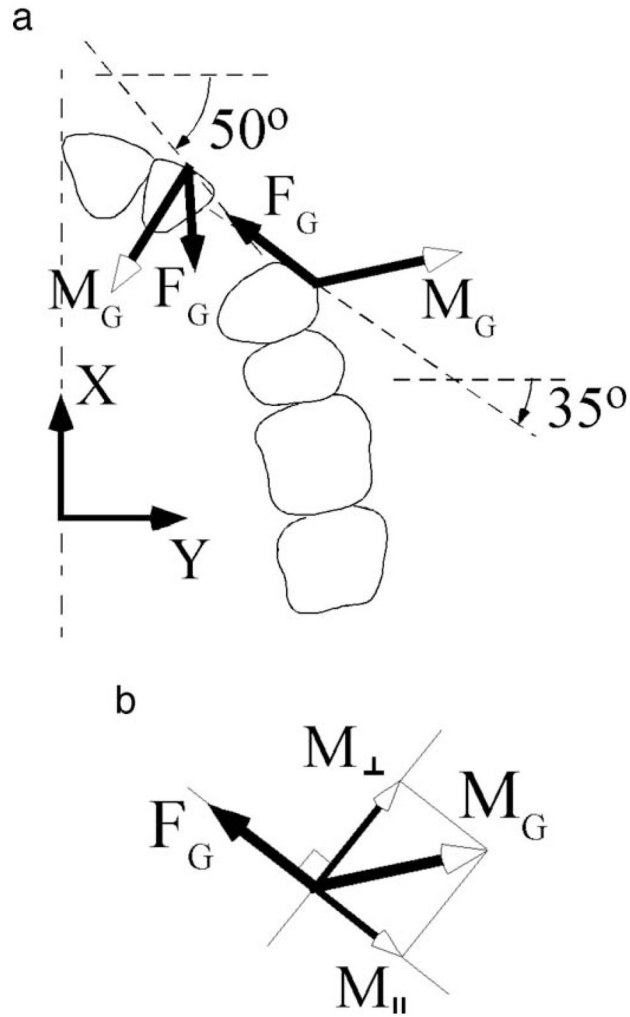
Figure 9.
(a) For the desired tooth translations, each $\mathbf{F}_G$ must approximate its y'-axis. With an appropriate $\mathbf{F}_G$, as on the canine for example, to counteract its tipping action, (b) there must be a component of $\mathbf{M}_G$, $M_\perp$, which is perpendicular to the force. $M_\parallel$ is the component of $\mathbf{M}_G$ that is parallel to $\mathbf{F}_G$.
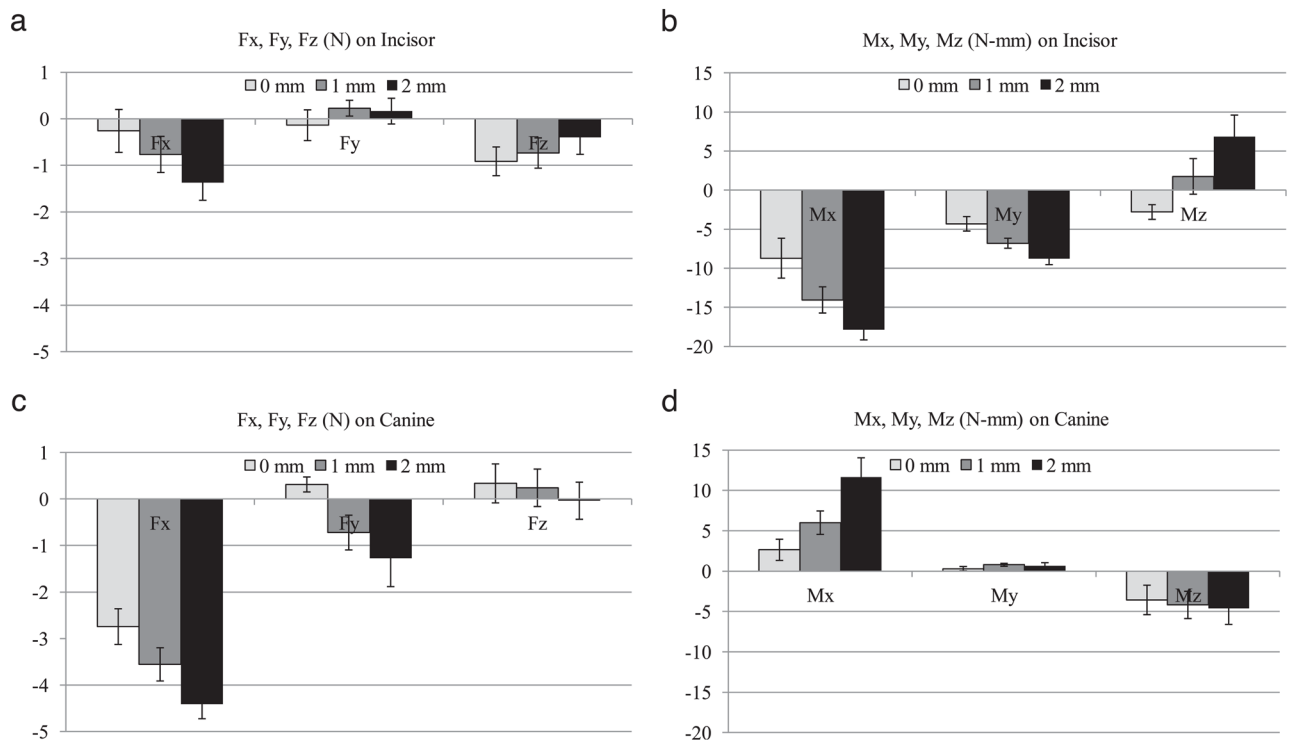
Figure 10.
Traditional presentation of force and moment components on the brackets produced by the first loop design. The results for 0, 1, and 2 mm of activations on the (a and b) incisor and (d and e) canine.
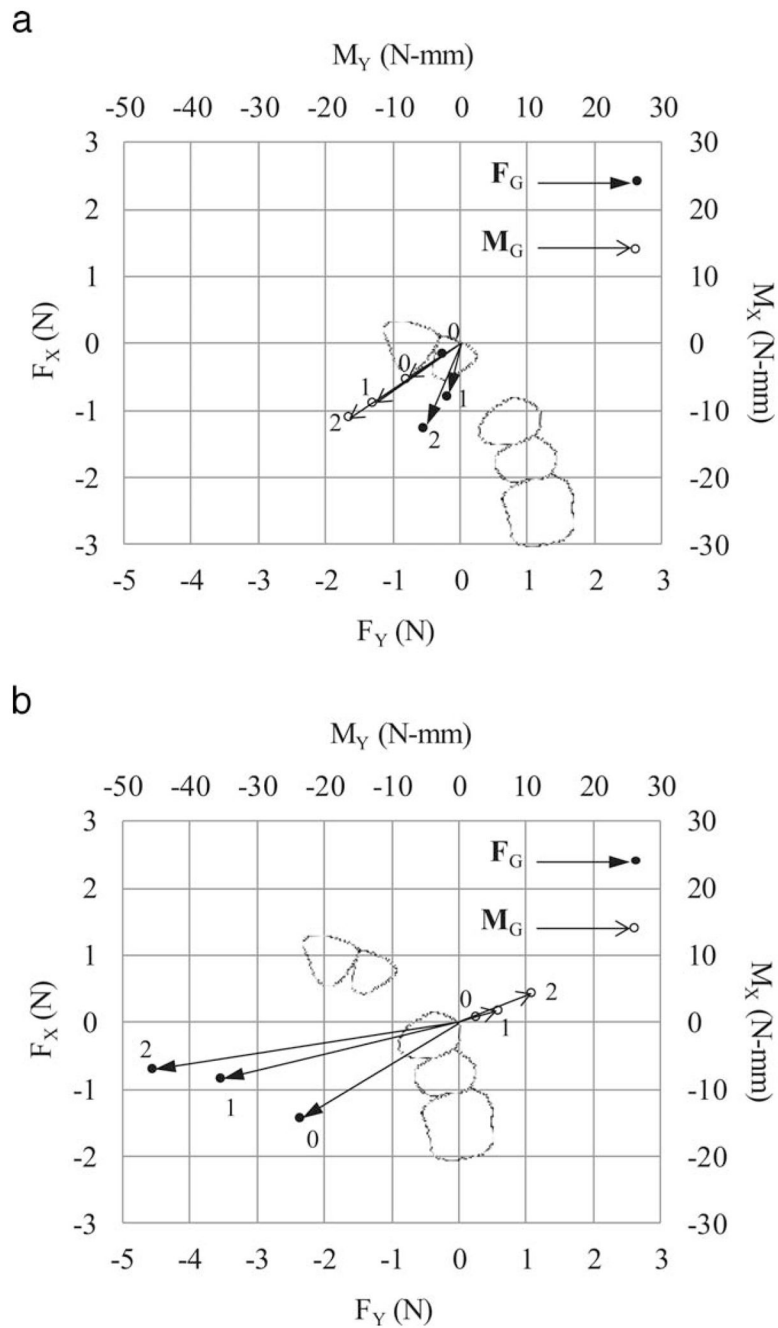
Figure 11.
The same data as in Figure 10, but as vectors ($\mathbf{F}_G$ and $\mathbf{M}_G$) projected onto the occlusal plane for the (a) incisor and (b) canine. The 0, 1, and 2 indicate activations in mm.

Figure 12.
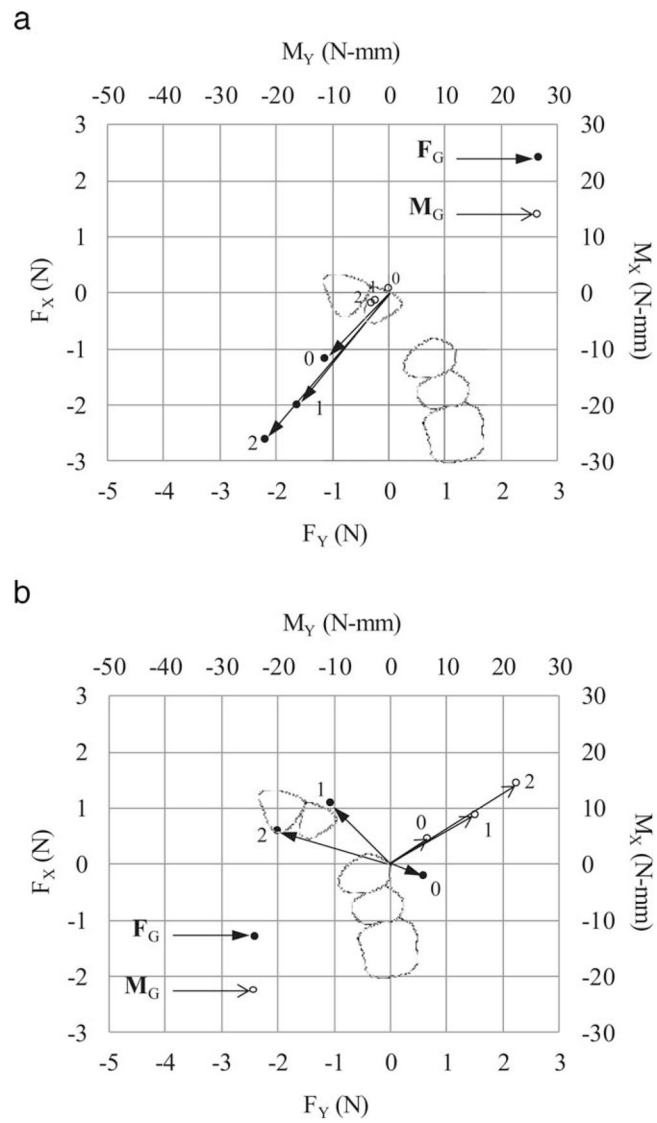As in Figure 11 but for the second loop design.

Table 1

M_x/F_x	M_y/F_x	M_z/F_x
M_x/F_y	M_y/F_y	M_z/F_y
M_x/F_z	M_y/F_z	M_z/F_z